

# Fractal Dimension of the Cantor Moiré Structures

Luciano Zunino\* and Mario Garavaglia

*Centro de Investigaciones Ópticas (CIOp), CC. 124 Correo Central, 1900 La Plata, Argentina.*

*Departamento de Física, Facultad de Ciencias Exactas, Universidad Nacional de La Plata (UNLP), 1900 La Plata, Argentina.*

---

## Abstract

In a recently published paper (J. of Modern Optics 50 (9) (2003) 1477-1486) a qualitative analysis of the moiré effect observed by superposing two grids containing Cantor fractal structures was presented. It was shown that the moiré effect is sensible to variations in the order of growth, dimension and lacunarity of the Cantor fractal. It was also verified that self-similarity of the original fractal is inherited by the moiré pattern.

In this work it is shown that these Cantor moiré structures are also fractals and the fractal dimension associated with them is theoretically determined and experimentally measured attending the size of rhombuses in the different orders of growth.

*Key words:* moiré, fractals, Cantor fractals, fractal dimension

*PACS:* 05.45.Df, 42.30.Ms

---

## 1 INTRODUCTION

### 1.1 Fractals

In recent years the study of fractals has attracted a lot of attention because many physical phenomena and natural structures can be analysed and de-

---

\* Corresponding author.

*Email addresses:* [lucianoz@ciop.unlp.edu.ar](mailto:lucianoz@ciop.unlp.edu.ar) (Luciano Zunino),  
[garavagliam@ciop.unlp.edu.ar](mailto:garavagliam@ciop.unlp.edu.ar) (Mario Garavaglia).

scribed by using a fractal approach [1]. B. B. Mandelbrot introduced the term fractal, which comes from the Latin *fractus* meaning broken, to describe irregular structures which are impossible to study using traditional Euclidean geometry. As he suggested, the principal characteristic of these new structures is their self-similarity: they are invariant under change of scale and displacement. A fractal is a set whose parts resemble the whole. This self-similarity can be mathematical or statistical. In the first case exact copies of the whole are obtained when the structure is viewed under magnification. These fractals are constructed through an iterative process of replacements of an object by  $n$  copies of itself, each one of which is scaled by an  $r < 1$  factor. Given a self-similar structure, there is a relation between the scaling factor  $r$  and the number  $n$  of pieces in which it is divided, according to the formula:

$$n = \frac{1}{r^{d_s}}, \quad (1)$$

where  $d_s$  is the called similarity dimension. Fractal dimensions provide a description of how much space the set fills.

The classic triadic Cantor fractal is an example of these structures. In its build-up process a sequence of closed intervals is generated, one after the zero step, two after the first step, four after the second, eight after the third, and so on. In general there will be  $2^k$  intervals of longitude  $1/3^k$  after the  $k^{th}$  step. Each iteration represents an order of growth. The Cantor fractal is defined as the array of points that remain after an infinite process of removals. In Fig. 1 are shown grids constructed following the first five orders of the triadic Cantor fractal ( $n = 2$  and  $r = 1/3$ ). It has been drawn with a finite height to aid the viewing.

**[Insert figure 1 about here]**

A mathematical fractal is obtained by considering the structure that results when the order of growth  $k \rightarrow \infty$ . Practical fractals are self-similar over a limited range of magnification and they are more appropriately referred as pre-fractals. However, in this paper, the term fractal will be applied to structures with finite  $k$ .

Fractals, as it was mentioned, can also be obtained using a statistical process. The similarity dimension is not meaningful for this class of fractals. However, there are other definitions of dimension that are defined for any set. The Hausdorff dimension, which is based on measures, is the oldest and probably the most important. Box-counting or box dimension (also known as Kolmogorov entropy, entropy dimension, capacity dimension and information dimension) is another dimension very popular in physical applications.

In this work the focus is on strictly self-similar fractals. The Hausdorff dimen-

sion equals the similarity dimension for self-similar fractals [2].

## 1.2 Moiré effect

In order to characterize fractal structures, optical diffraction and scattering by fractal openings is being increasingly studied [3, 4, 5]. A complete list of references can be found in Ref. [5]. It allows the properties and parameters that characterize these objects to be determined.

More recently another powerful optical tool, the moiré effect, was applied to this particular geometry [6, 7]. Moiré patterns are observed when two similar screens or sets of rulings are nearly superposed. They may be described as the locus of points of intersection of the two overlapping grids, as it is shown in Fig. 2. Assume that each of the two original grids can be regarded as an indexed family of lines. Then, the resulting moiré patterns are most pronounced when the indices of the intersections satisfy certain simple relations. This is known as the indicial representation method for the determination of the moiré patterns [8], which could be called algebraic method.

**[Insert figure 2 about here]**

There are other methods to determine characteristics of moiré patterns using different approaches: geometric [9], analytic [10], vector [11], tensor [12], autocorrelation [13], Fourier transformation [14], and by using a description of the superposed grids according to Walsh functions [15]. These approaches could be a sequence initiated as early as 1874 by Lord Rayleigh –who was the first to explain how moiré patterns are observed from the superposition of two families of equispaced parallel straight lines [16]–, and continues to date.

A Ronchi grid can be described as  $G(x, y, d, \phi)$  by the expression:

$$G(x, y, d, \phi) = \sum_{n=1}^N \text{rect} \left\{ \frac{[x - nd - \phi(x, y)]}{d/2} \right\}, \quad (2)$$

where  $x$  is the variable over which the rectangular function describes the Ronchi grid distribution,  $y$  the variable that permits describing the grid  $G(x, y, d, \phi)$  in the plane  $(x, y)$ ,  $d$  the grid period and  $\phi$  the phase of the grid considered as its first line position respect to the left border of the reference frame. Formally, the bidimensional Ronchi grid can be represented as the Cartesian product  $G = ExR$ , being  $E$  a straight line segment parallel to the y-axis of coordinates and  $R$  the rectangular function in the x-axis of coordinates. Different operators can be applied to the function  $G(x, y, d, \phi)$ , such as translation  $T(x, y)$  over the plane  $(x, y)$ , scaling  $S(x, y)$  that produces a variation of the original period  $d$ , and rotation  $A(\alpha)$  of the grid around its  $z$  axis in a certain angle  $\alpha$ .

Finally, the superposition of the original grid  $G(x, y, d, \phi)$  with the modified grid  $G'(x, y, d, \phi)$ , generated by the application of the operators  $T(x, y)$ ,  $S(x, y)$ , and  $A(\alpha)$ , or any of them, over  $G(x, y, d, \phi)$ , allows determining, for example, the transmittance  $t(x, y)$  of the moiré pattern by means of the correlation  $G * G'$ , according to:

$$t(x, y) = \int_{-\infty}^{\infty} \int_{-\infty}^{\infty} G(x, y, d, \phi) G'(x, y, d, \phi) dx dy. \quad (3)$$

When referring to the appearance of the moiré phenomenon, the verbal form “visual” is often used to describe the observation of the emerging geometrical figures called moiré patterns. It seems to be a little reductionistic approach to describe it, because not only eyes observe moiré patterns. In fact, any type of image capture system can be successfully utilized to capture moiré patterns and to display them to be visually observed. Actually, moiré patterns can be photographed, photocopied, taken by TV camera, PC designed and scanned, and, after some appropriate processes is applied to the captured information, they can be visually observed. Different types of display support are employed, as paper reproduced pictures, projected slides or transparencies, photocopies, paper printed images, TV and monitor screen images, etc. However, it is convenient to mention that all detectors and displays listed above are discrete in nature and finite in size. They have their proper structure. Then, the bidimensional correlation function for detectors is limited by the macroscopic dimensions of the devices ( $X_M$ ) and the microscopic dimensions of its sensible components ( $X_m$ ) as shown in Fig. 3.

**[Insert figure 3 about here]**

Then the best matching between moiré patterns and the structure of detectors must be accomplished to assure the clearest observation of them and avoid the appearance of the noisy aliasing effect [17]. Also, the best observation of moiré fringes is strongly limited by the poor capacity of the eye to distinguish very low and very high spatial frequency components in an image. Finally, the observation of moiré patterns is related with local and global correlations of signals in the visual system [18].

Moiré patterns are obtained from different types of 2D grids: equispaced parallel lines—as in Fig. 2—, parallel lines of variable spacing, radial lines, circles whose difference between consecutives radii is constant, zone plates, parabolas, spirals, etc. It has been shown that the moiré effect is also present after superposing a Cantor bidimensional structure over its own replica rotated in a small angle. It was also verified that self-similarity of the original fractal is inherited by the moiré pattern [6]. In order to illustrate this property, Fig. 4 shows the moiré fringes obtained by superposing the triadic Cantor fractals

of orders  $k = 4$ ,  $k = 5$  and  $k = 6$ . In all the moiré figures the fractal structures are superposed over their replicas, which have been rotated an angle of  $10^\circ$ . It is observed that the moiré patterns contain tinier and more complex structures as the order of growth increases. The central parts of the moiré patterns for orders of growth  $k = 5$  and  $k = 6$  were magnified to observe the structure in detail. The features in the magnified region directly correspond to the characteristic moiré features of the precedent order. So the moiré patterns inherit the self-similarity of the original Cantor structures.

**[Insert figure 4 about here]**

Now, in this work it will be analysed if these Cantor moiré structures are fractals. To our knowledge this problem has not been introduced before.

The use of the term triadic Cantor fractal is, strictly, an abuse of language, since in fact what is superposed is the structure which results of extending the triadic Cantor perpendicularly within the  $2D$  plane. However, it is a  $1D$  geometry because it only has full freedom in one dimension, while its other dimension is completely determined. Then, it is possible to consider it as the Cartesian product  $C = ExF$ :

$$C = ExF = \{(x, y) : x \in E, y \in F\}, \quad (4)$$

where  $E$  is a straight line segment and  $F$  is the triadic Cantor set. It was shown [19] that this structure has Hausdorff dimension:

$$\dim_H C = \dim_H (ExF) = \dim_H E + \dim_H F = 1 + \frac{\ln 2}{\ln 3}. \quad (5)$$

## 2 Analysis

The superposition of bidimensional structures to generate the moiré effect is expressed by the logical operation of intersection  $\cap$ , which can be quantified by means of the analytical operation of correlation of the mathematical functions that describe the structures.

In order to visualize the intersection between the two Cantor moiré structures the following elementary algebra concept is applied:

$$A \cap B = (A^c \cup B^c)^c. \quad (6)$$

The moiré structure corresponds to the complement region obtained from the union of the complement of the original structures. In Fig. 5 it is illustrated this operation for the triadic Cantor fractal with order of growth  $k = 4$ .

[Insert figure 5 about here]

Now, it is easy to follow the behaviour of the moiré when the order of growth is increased. Figure 6 shows the intersection regions for the orders of growth  $k = 3$ ,  $k = 4$  and  $k = 5$ .

[Insert figure 6 about here]

As the order of growth is increased the original rhombuses that result from the intersection are divided in new four small rhombuses with length size scaled by a factor  $r = 1/3$ . So, it is possible to conclude that the similarity dimension of the moiré structures is:

$$d_s = \frac{\ln 4}{\ln 3} = 2 \frac{\ln 2}{\ln 3}. \quad (7)$$

A justification of this result can be achieved by analysing the intersection formula for fractals. The following two theorems are used [20]:

*Theorem A.* If  $A, B$  are Borel subsets of  $\mathbb{R}^n$  and  $\sigma$  ranges over a group  $G$  of transformations, such as the group of translations, congruences or similarities then:

$$\dim_H (A \cap \sigma(B)) \leq \max \{0, \dim_H (Ax B) - n\},$$

for almost all  $x \in \mathbb{R}^n$ .

*Theorem B.* Let  $A, B \subset \mathbb{R}^n$  be Borel sets, and let  $G$  be a group of transformations on  $\mathbb{R}^n$ . Then:

$$\dim_H (A \cap \sigma(B)) \geq \dim_H A + \dim_H B - n,$$

for a set of motions  $\sigma \in G$  of positive measure in the following cases:

- (a)  $G$  is the group of similarities and  $A$  and  $B$  are arbitrary sets;
- (b)  $G$  is the group of rigid motions,  $A$  is arbitrary and  $B$  is a rectifiable curve, surface, or manifold;
- (c)  $G$  is the group of rigid motions and  $A$  and  $B$  are arbitrary, with either  $\dim_H A > \frac{1}{2}(n+1)$  or  $\dim_H B > \frac{1}{2}(n+1)$ .

Remember that a rigid motion or direct congruence may be achieved by a combination of a rotation and a translation. It does not involve reflection.

The Cantor moiré structures have  $A = B = C = ExF$ ,  $n = 2$  and  $\sigma$  a rotation. Then:

$$\dim_H (C \cap \sigma(C)) \leq \max \{0, \dim_H (Cx C) - 2\}, \quad (8)$$

and

$$\dim_H (C \cap \sigma(C)) \geq 2 \dim_H C - 2 = 2 \left( 1 + \frac{\ln 2}{\ln 3} \right) - 2 = 2 \frac{\ln 2}{\ln 3}. \quad (9)$$

But  $\dim_H (Cx C) = 2 \dim_H C = 2 [1 + (\ln 2/\ln 3)]$  [21], so the following upper bound is obtained:

$$\dim_H (C \cap \sigma(C)) \leq \max \{0, \dim_H (Cx C) - 2\} = \max \left\{ 0, 2 \frac{\ln 2}{\ln 3} \right\} = 2 \frac{\ln 2}{\ln 3} \quad . \quad (10)$$

Then, according to the results in equation (9) and (10) the Hausdorff dimension of the Cantor moiré structures straightforward equals to  $2 \ln 2/\ln 3$ .

It is possible another explanation of this result by analysing the Cartesian product  $F \times F$ , where  $F$  is the triadic Cantor fractal. Figure 7 shows this product. It was shown [22] that this Cartesian Cantor product has a Hausdorff dimension exactly  $2 \ln 2/\ln 3$ .

**[Insert figure 7 about here]**

The Cantor moiré structure is obtained under a bi-Lipschitz transformation  $f$  of this Cartesian product, i.e.:

$$f : X \rightarrow Y, \quad c_1 |x - y| \leq |f(x) - f(y)| \leq c_2 |x - y|, \quad (x, y \in X), \quad (11)$$

for  $0 < c_1 \leq c_2 < \infty$ . Furthermore, the Hausdorff dimension is invariant under bi-Lipschitz transformation [23]. Then, it is confirmed that the Hausdorff dimension of the new structure is  $2 \ln 2/\ln 3$ .

It is easy to extend these results to other Cantor sets. Figure 8 shows the septic Cantor bars ( $n = 4$  and  $r = 1/7$ , being  $d = \ln 4/\ln 7$ ) in their first four orders of growth.

**[Insert figure 8 about here]**

The intersection regions associated to this fractal for the orders of growth  $k = 1$ ,  $k = 2$  and  $k = 3$  are shown in Fig. 9. The original rhombuses are divided in new sixteen small rhombuses with length size scaled by a factor  $r = 1/7$ . Then,

$$d_s = \frac{\ln 16}{\ln 7} = 2 \frac{\ln 4}{\ln 7}, \quad (12)$$

as it was expected.

**[Insert figure 9 about here]**

### 3 Conclusions

It can be concluded that the Cantor moiré structures are self-similar fractals with twice the similarity and Hausdorff dimension of the original Cantor structures.

The extension of these results to other fractal constructions is of great importance because new fractal structures can be obtained. The intention is to demonstrate that one way of constructing ‘new fractals from old’ is by forming moiré with them\* .

### Acknowledgements

Luciano Zunino thanks for the doctoral research fellowship from Consejo Nacional de Investigaciones Científicas y Técnicas (CONICET), Argentina, during the research period.

### References

- [1] B. B. Mandelbrot, *The Fractal Geometry of Nature*, W. H. Freeman, New York, 1982.
- [2] J. Feder, *Fractals*, Plenum Press, New York, 1988, in particular, see page 19.
- [3] C. Allain, M. Cloitre, Optical diffraction on fractals, *Phys. Rev. B* 33 (1986) 3566–3569.
- [4] C. Allain, M. Cloitre, Spatial spectrum of a general family of self-similar arrays, *Phys. Rev. A* 36 (1987) 5751–5757.
- [5] L. Zunino, M. Garavaglia, Fraunhofer diffraction by Cantor fractals with variable lacunarity, *J. of Modern Optics* 50 (5) (2003) 717–727.
- [6] L. Zunino, M. Garavaglia, Moiré by fractal structures, *J. of Modern Optics* 50 (9) (2003) 1477–1486.
- [7] D. Calva Méndez, M. Lehman, Moire effect for the superposition of two Cantor gratings, *Proc. SPIE* 4829 (2002) 355–356, 19th Congress of the International Commission for Optics: Optics for the Quality of Life; Giancarlo C. Righini, Anna Consortini Eds.
- [8] G. Oster, M. Wasserman, C. Zwerling, Theoretical interpretation of moire patterns, *J. Opt. Soc. Am.* 54 (1964) 169–175.

---

\* It is reproduced the following phrase “One way of constructing ‘new fractals from old’ is by forming Cartesian products” [24] but modified for the new situation.



- [9] D. Tolenaar, Moiré interferentieverschijnselen bij rasterdruck, Tech. rep., Instituut voor Garphische Techniek, Amsterdam (1945).
- [10] V. Ronchi, La prova dei sistema ottici (Italian), *Attualità Scientifici* 37, N. Zanichelli, Bologna.
- [11] C. A. Sciammarella, Holographic moiré, an optical tool for the determination of displacements, strains, contours, and slopes of surfaces, *Optical Engineering* 21 (1982) 447–457.
- [12] P. Tatasciore, E. K. Hack, Projection moiré: using tensor calculus for general geometries of optical setups, *Optical Engineering* 34 (1995) 1887–1899.
- [13] L. Alqazzaz, G. L. Rogers, Coding and decoding of dilute and continuous-tone objects in incoherent light, *J. Opt. Soc. Am.* 65 (1975) 695–699.
- [14] I. Amidror, A Generalized Fourier-based Method for the Analysis of 2D Moiré Envelope-forms in Screen Superpositions, *J. of Modern Optics* 41 (1994) 1837–1862.
- [15] C. Colautti, O. Trabocchi, E. E. Sicre, Moire properties of Walsh functions, *Optics & Laser Technology* 29 (1997) 261–265.
- [16] J. W. Strutt (Lord Rayleigh), On the manufacture and theory of diffraction gratings, *Philosophical Magazine* 47 (1874) 81–93 and 193–205.
- [17] B. W. Bell, C. L. Koliopoulos, Moire topography, sampling theory, and charged-coupled devices, *Optics Lett.* 9 (1984) 171–173.
- [18] D. Marr, *Vision: A computational investigation into the human representation and processing of visual information*, Freeman, San Francisco, 1982.
- [19] K. J. Falconer, *Fractal Geometry: Mathematical Theory and Applications*, John Wiley & Sons, New York, 1990.
- [20] See reference [19] at pages 102-103.
- [21] See reference [19] at pages 56 and 95; in particular see Example 4.3 and Corollary 7.4.
- [22] See reference [19] at pages 93-96.
- [23] See reference [19] at page 30.
- [24] See reference [19] at page 92.



Fig. 1. Grids constructed following the first five orders of growth for the triadic Cantor fractal ( $n = 2$  and  $r = 1/3$ ).

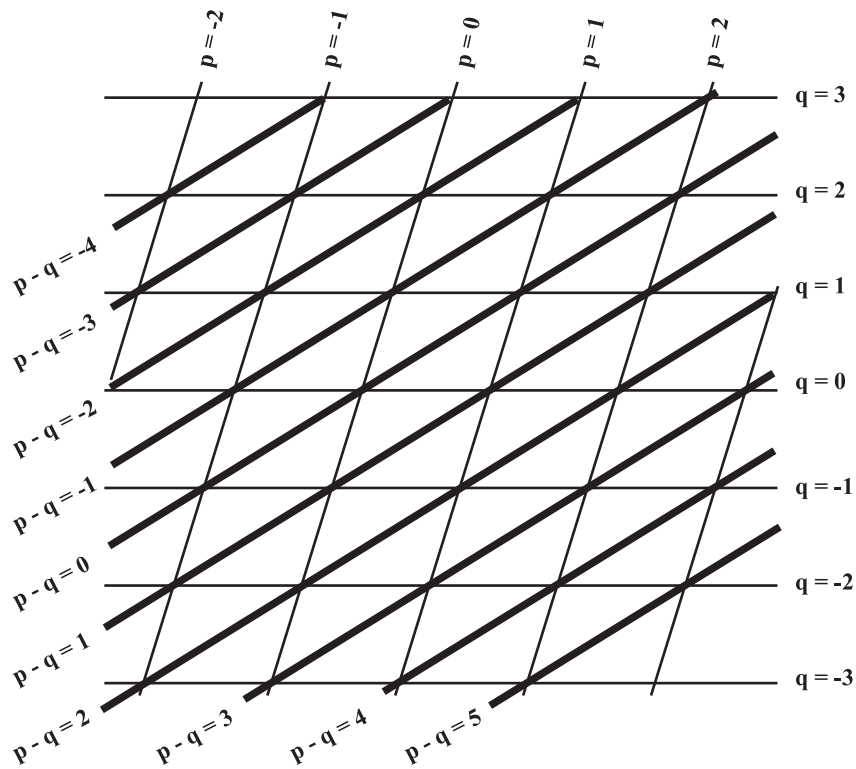


Fig. 2. Moiré pattern generated by superposition of two grids;  $p$  and  $q$  are the indices of both families of lines. Moiré fringes are represented by  $p - q = 0, \pm 1, \pm 2, \dots$ .

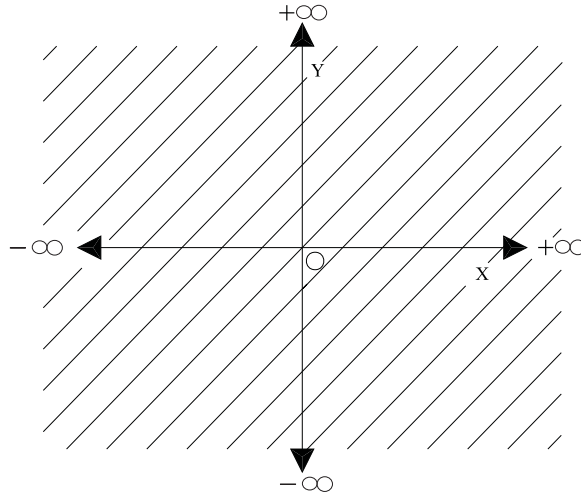


Figure 3 a)

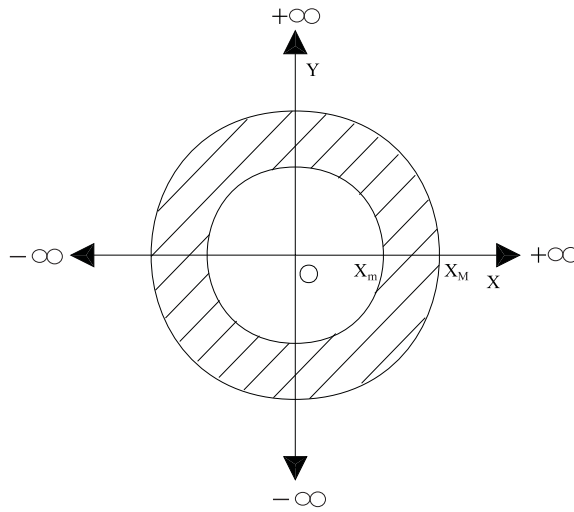


Figure 3 b)

Fig. 3. a) The bidimensional correlation function is defined in such a way that must be integrated over the entire plane, from  $-\infty$  to  $+\infty$ . b) The bidimensional correlation function for detectors is limited by the macroscopic dimensions of the devices ( $X_M$ ) and the microscopic dimensions of its sensible components ( $X_m$ ).

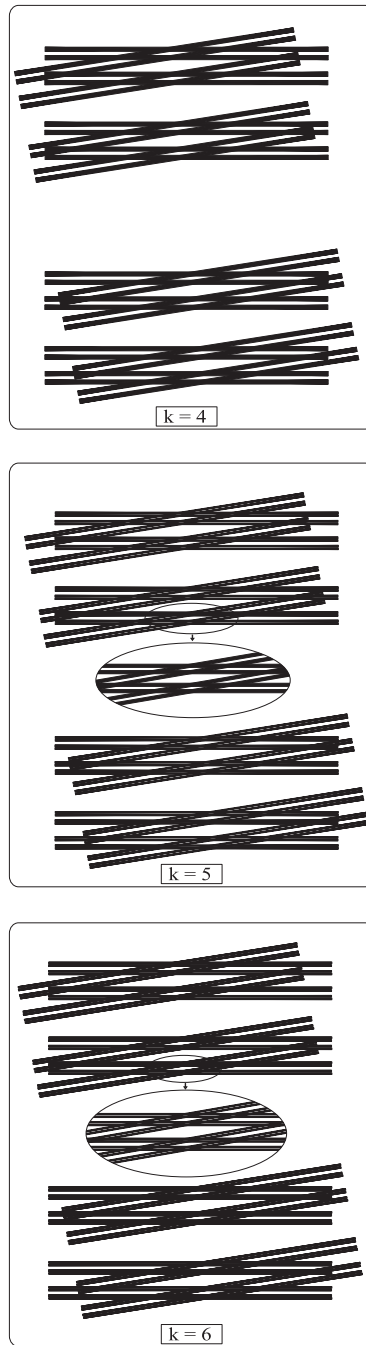


Fig. 4. Moiré patterns superposing triadic Cantor fractals ( $n = 2$  and  $r = 1/3$ ) for the orders of growth  $k = 4$  (upper figure),  $k = 5$  (central figure), and  $k = 6$  (lower figure).

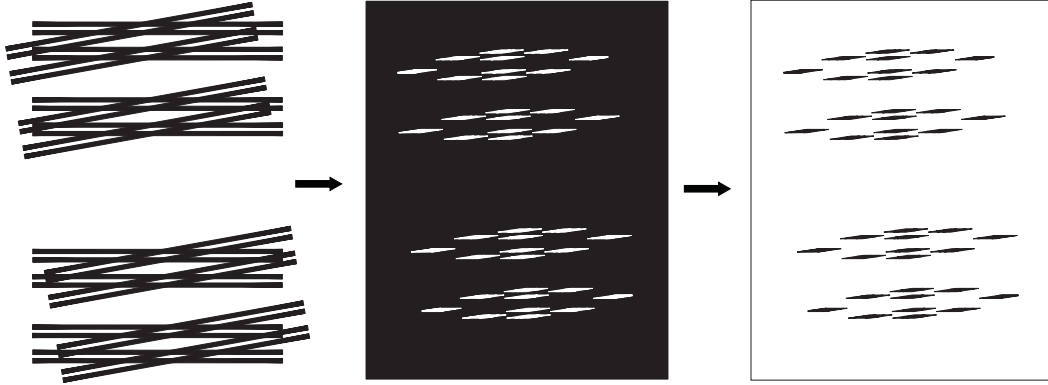


Fig. 5. Operations introduced in order to visualize the intersection regions (triadic Cantor fractal, order of growth  $k = 4$ ).

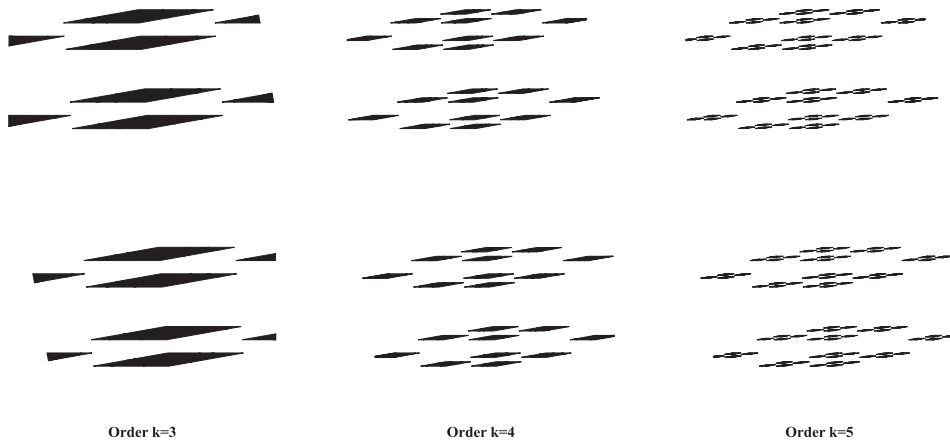


Fig. 6. Intersection regions of the triadic Cantor fractals for the orders of growth  $k = 3$  (left figure),  $k = 4$  (central figure), and  $k = 5$  (right figure).

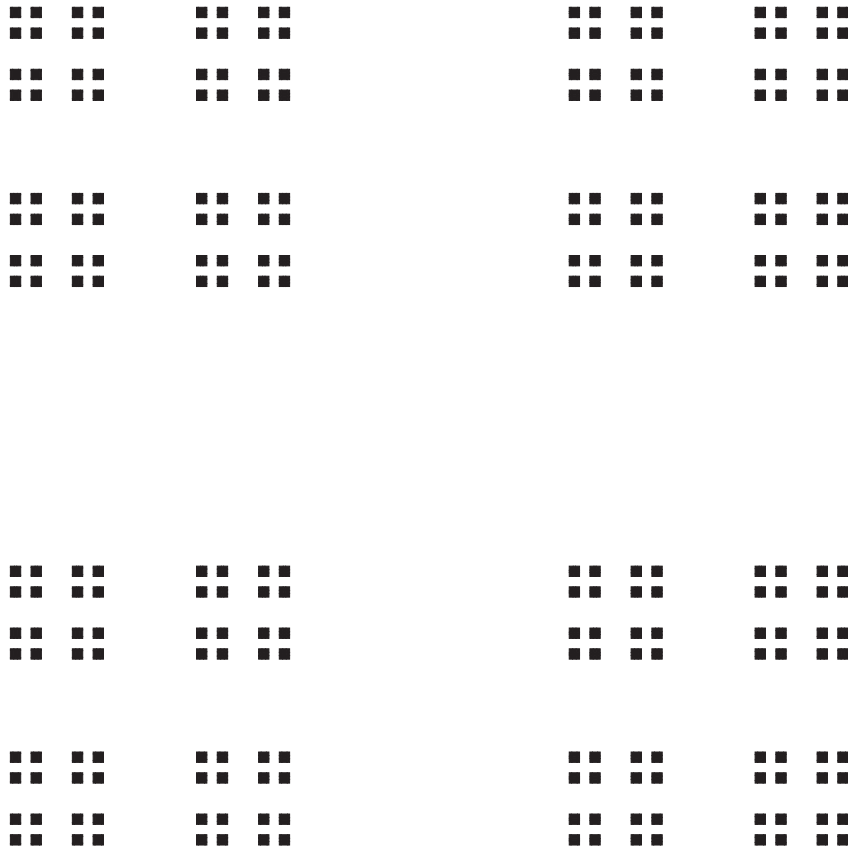


Fig. 7. Cartesian product of the triadic Cantor fractal with itself for the order of growth  $k = 4$ .

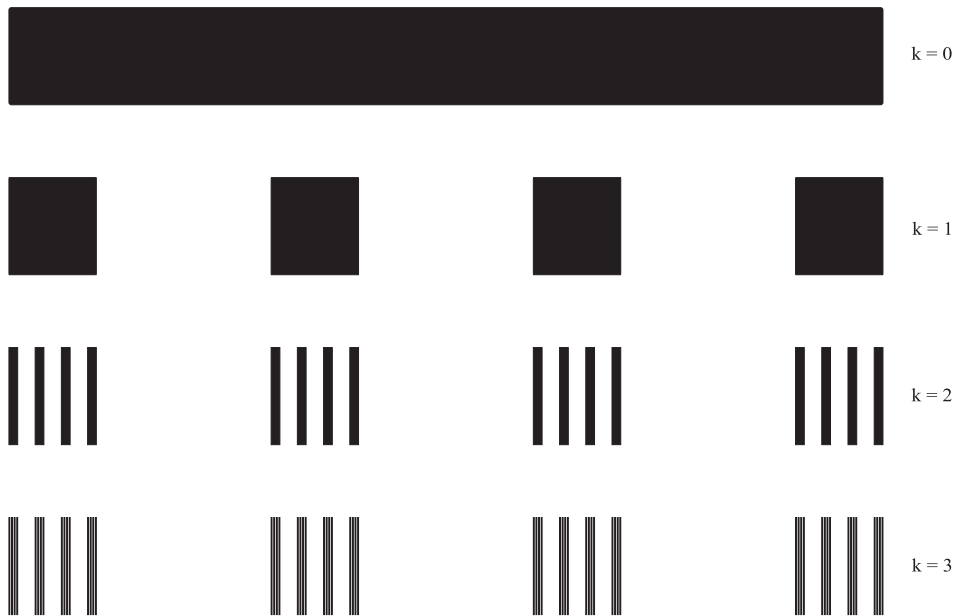


Fig. 8. Grids constructed following the first orders of growth of the septic Cantor fractal ( $n = 4$  and  $r = 1/7$ ).

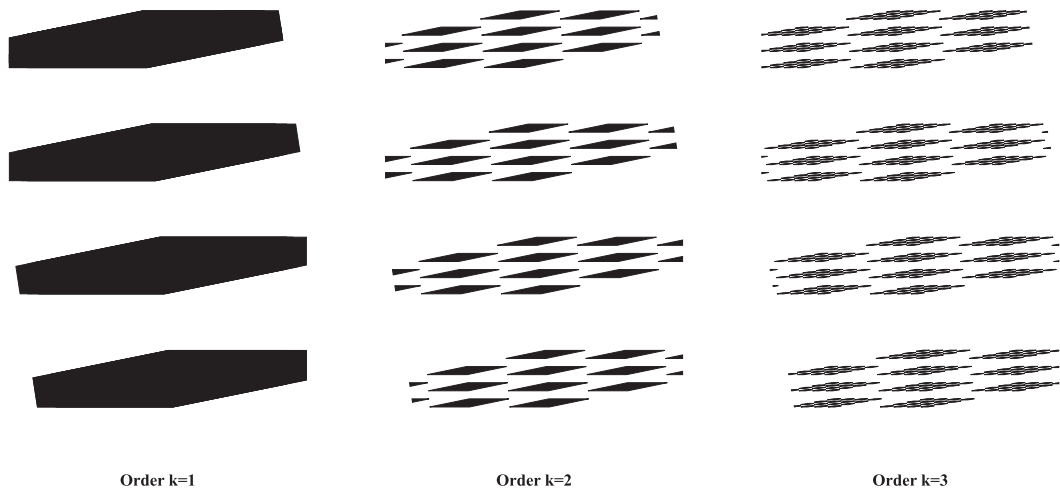


Fig. 9. Intersection regions of the septic Cantor fractals for the orders of growth  $k = 1$  (left figure),  $k = 2$  (central figure), and  $k = 3$  (right figure).